Metal-to-Metal Silyl Migration and Silicon−Carbon Bond Cleavage/Re-formation Processes in the Methylene/Silyl Complexes $Cp^*_2Ru_2(\mu\text{-}CH_2)(SiR_3)(\mu\text{-}Cl)$

Quinetta D. Shelby, Wenbin Lin, and Gregory S. Girolami*

School of Chemical Sciences, The University of Illinois at Urbana−Champaign, 600 South Mathews Avenue, Urbana, Illinois 61801

Received March 4, 1999

Ruthenium methylene/silyl complexes of stoichiometry $Cp^*_2Ru_2(\mu\text{-}CH_2)(SiR_3)(\mu\text{-}Cl)$, where $SiR_3 = SiMe_3$ (**1**), $SiEt_3$ (**2**), $SiMe_2Et$ (**3**), and $SiMe_2Ph$ (**4**), are produced when $[Cp^*RuCl]_4$ is treated with the appropriate dialkylmagnesium reagent, $Mg(CH_2SiR_3)_2$. Each complex undergoes two fluxional processes as observed by variable-temperature ^1H NMR spectroscopy. The low-temperature exchange process is migration of the SiR_3 unit from one Ru center to the other, whereas the high-temperature process is the reversible re-formation of the C−Si bond between the silyl group and the bridging methylene unit. The activation parameters for the low-temperature exchange process in **1**−**4** are sensitive to the nature of the silyl group: $\Delta H^‡$ becomes smaller and $\Delta S^‡$ becomes more negative if the SiR_3 group bears nonidentical or larger, more flexible substituents. This finding suggests that the transition state for this exchange process is crowded or characterized by different amounts of solvent reorganization depending on the SiR_3 group involved. In contrast, the activation parameters for the high-temperature process in **1**−**4** are relatively independent of the nature of the silyl ligand. The small variation in the activation parameters for reformation of the C−Si bond is consistent with a noncrowded transition state in which the solvent reorganization is relatively independent of the nature of the SiR_3 group.

Introduction

Intramolecular silyl migration processes in transition metal complexes are of current interest because of their role in catalytic and synthetic chemistry. For example, such reactions are at the heart of catalytic alkene hydrosilation reactions[1,2] and are key steps in the $RuHCl(CO)(PPh_3)_2$-catalyzed cross-disproportionation of vinyl silanes and monosubstituted alkenes.[3] For stoichiometric reactions, several kinds of silyl migration processes have been noted. Among these are migration of metal-bound silyl groups to ligands such as alkenes,[4−7] silenes,[8] alkynes,[9−11] alkylidenes,[12] carbon monoxide,[13−16] isonitriles,[15,16] and cyclopentadienyl groups.[17−19]

Several years ago, we described the synthesis of the methylene/silyl complex $Cp^*_2Ru_2(\mu\text{-}CH_2)(SiMe_3)(\mu\text{-}Cl)$, **1**, by treatment of $[Cp^*RuCl]_4$ with the dialkylmagnesium reagent $Mg(CH_2SiMe_3)_2$.[20] In this reaction, the CH_2-SiMe_3 bond is cleaved, and both fragments are retained in the organometallic product. The variable-temperature ^1H and ^{13}C NMR spectra showed that **1** undergoes *two different* silyl migration processes. The low-temperature process exchanges the two Cp* groups and was proposed to involve hopping of the silyl group between the two metal centers. The high-temperature process exchanges the inequivalent protons of the bridging methylene group and was proposed to involve re-formation of the C−Si bond between the methylene and silyl groups.

Although other mechanisms can be written that would exchange the diastereotopic methylene protons,[21]

(1) Ojima, I. In *The Chemistry of Organic Silicon Compounds*; Patai, S., Rappoport, Z., Eds.; Wiley: New York, 1989; Chapter 25.
(2) Braunstein, P.; Knorr, M.; Hirle, B.; Reinhard, G.; Schubert, U. *Angew. Chem., Int. Ed. Engl.* **1992**, *31*, 1583−1585.
(3) Wakatsuki, Y.; Yamazaki, H.; Nakano, M.; Yamamoto, Y. *J. Chem. Soc., Chem. Commun.* **1991**, 703−704.
(4) Fryzuk, M. D.; Rosenberg, L.; Rettig, S. J. *Organometallics* **1996**, *15*, 2871−2880.
(5) Procopio, L. J.; Carroll, P. J.; Berry, D. H. *J. Am. Chem. Soc.* **1991**, *113*, 1870−1872.
(6) Arnold, J.; Engeler, M. P.; Elsner, F. H.; Heyn, R. H.; Tilley, T. D. *Organometallics* **1989**, *8*, 2284−2286.
(7) Randolph, C. L.; Wrighton, M. S. *J. Am. Chem. Soc.* **1986**, *108*, 3366−3374.
(8) Procopio, L. J.; Berry, D. H. *J. Am. Chem. Soc.* **1991**, *113*, 4039−4040.
(9) Esteruelas, M. A.; Oro, L. A.; Valero, C. *Organometallics* **1991**, *10*, 462−466.
(10) Ojima, I.; Ingallina, P.; Donovan, R. J.; Clos, N. *Organometallics* **1991**, *10*, 38−41.
(11) Tanke, R. S.; Crabtree, R. H. *J. Chem. Soc., Chem. Commun.* **1990**, 1056−1057.
(12) Berry, D. H.; Koloski, T. S.; Carroll, P. J. *Organometallics* **1990**, *9*, 2952−2962.
(13) Knorr, M.; Braunstein, P.; Tiripicchio, A.; Ugozzoli, F. *Organometallics* **1995**, *14*, 4910−4919.
(14) Knorr, M.; Braunstein, P.; DeCian, A.; Fischer, J. *Organometallics* **1995**, *14*, 1302−1309.
(15) Elsner, F. H.; Tilley, T. D.; Rheingold, A. L.; Geib, S. J. *J. Organomet. Chem.* **1988**, *358*, 169−183.
(16) Campion, B. K.; Falk, J.; Tilley, T. D. *J. Am. Chem. Soc.* **1987**, *109*, 2049−2056.
(17) Berryhill, S. R.; Corriu, R. J. P. *J. Organomet. Chem.* **1989**, *370*, C1−C4.
(18) Pannell, K. H.; Vincenti, S. P.; Scott, R. C., III *Organometallics* **1987**, *6*, 1593−1594.
(19) Pasman, P.; Snel, J. J. M. *J. Organomet. Chem.* **1986**, *301*, 329−335.
(20) Lin, W.; Wilson, S. R.; Girolami, G. S. *Organometallics* **1994**, *13*, 2309−2319.

10.1021/om990156b CCC: $18.00
Publication on Web 04/21/1999

Table 1. ^{1}H NMR Spectroscopic Data for 2−4[a]

assignment	2	3	4
$SiMe_2$		0.62(s)	0.73 (s)
$SiMe_2$			0.86 (s)
$SiCH_2CH_3$	0.94 (q, $^3J_{HH} = 7.5$)	0.93 (m, $^3J_{HH} = 7.8$)	
$SiCH_2CH_3$	1.01 (q, $^3J_{HH} = 7.8$)		
$SiCH_2CH_3$	1.52 (t, $^3J_{HH} = 7.4$)	1.49 (t, $^3J_{HH} = 7.8$)	
C_5Me_5	1.33 (s)	1.36 (br)	1.34 (s)
C_5Me_5	1.60 (s)	1.62 (br)	1.44 (s)
p-CH			7.26 (t, $^3J_{HH} = 7.4$)
m-CH			7.39 (t, $^3J_{HH} = 7.4$)
o-CH			8.01 (d, $^3J_{HH} = 7.2$)
CH_2	10.27 (s)	10.00 (s)	10.22 (s)
CH_2	10.78 (s)	10.76 (s)	10.83 (s)

[a] All NMR spectra were taken at −90 °C in C_7D_8. Chemical shifts are reported in ppm and coupling constants in Hz.

several studies rule them out and provide convincing evidence for the reversible C−Si bond cleavage process proposed for the high-temperature exchange process. For instance, when **1** is treated with 4 equiv of PMe_3 or CO, the C−Si bond is re-formed to yield mononuclear products $Cp^*Ru(CH_2SiMe_3)L_2$ and Cp^*RuClL_2 where L = PMe_3 or CO. Further evidence that the $SiMe_3$ group in $Cp^*_2Ru_2(\mu\text{-}CH_2)(SiMe_3)(\mu\text{-}Cl)$ must participate in both the high- and low-temperature processes comes from the observation that $[Cp^*_2Ru_2(\mu\text{-}CH_2)(PMe_3)(\mu\text{-}Cl)^+]$, which is structurally and electronically similar to **1**, is nonfluxional up to 160 °C.

The low-temperature process seen for **1**, the reversible intramolecular migration of a silyl group from one metal to another, was the first reported example of such a process. Since then, reversible intramolecular metal-to-metal silyl transfer processes have been seen in a series of complexes of stoichiometry $Cp_2Ru_2(\mu\text{-}CH_2)(CO)_2(SiR_3)(H)$, where SiR_3 = $SiMe_3$, $SiEt_3$, $Si(n\text{-}Pr)_3$, $SiMe_2Ph$, $SiPh_3$, or $Si(OMe)_3$.[22] In addition, it has been shown that compounds of the type $(CO)_3(SiR_3)Fe(\mu\text{-}PPh_2)Pt(PPh_3)(CO)$, where SiR_3 = $Si(OMe)_3$ or $SiMe_2Ph$, rearrange *irreversibly* to give $(CO)_4Fe(\mu\text{-}PPh_2)Pt(PPh_3)(SiR_3)$.[2] The structural characterization of $Rh_2H_2\{P(i\text{Pr})_3\}_2(\mu\text{-}Cl)\{\mu\text{-}Si(p\text{-}FC_6H_4)_2\}\{\mu\text{-}Si(p\text{-}C_6H_4)_3\}$[23] and $[Li(thf)_4][Cu_5Cl_4\{Si(SiMe_3)_3\}_2]$,[24] both of which contain bridging tertiary silyl ligands, also adds credence to the proposed low-temperature mechanism.

The high-temperature process seen for **1**, a reversible Si−C bond re-formation process, is also rare in organotransition metal chemistry. There is one other example of a reversible α-silyl elimination process in an organotransition metal complex,[25] although in this compound, $Pt(CH_2SiMe_3)H[(t\text{-}Bu)_2PCH_2P(t\text{-}Bu)_2]$, the process is very slow and takes place over a period of 7 days at room temperature.

Herein we report the preparation of new analogues of **1** that contain silyl groups with various substituents. For each of these compounds, the activation parameters for both exchange processes have been measured and compared to shed light on the factors that affect the rates of the silyl migrations in these organometallic compounds.

Results

Synthesis and Properties of New Methylene/Silyl Diruthenium Complexes. We have previously reported that treatment of $[Cp^*RuCl]_4$ with an equimolar amount of the dialkylmagnesium reagent $Mg(CH_2SiMe_3)_2$ yields the unexpected product $Cp^*_2Ru_2(\mu\text{-}CH_2)(SiMe_3)(\mu\text{-}Cl)$ (**1**), in which the methylene and silyl ligands are generated by cleavage of a Si−C bond.[20] We now show that this reaction can be generalized: treatment of $[Cp^*RuCl]_4$ with other dialkylmagnesium reagents of the form $Mg(CH_2SiR_3)_2$ affords new diruthenium complexes with different substituents on the silicon atom. The new compounds we have made are $Cp^*_2Ru_2(\mu\text{-}CH_2)(SiR_3)(\mu\text{-}Cl)$, where SiR_3 = $SiEt_3$ (**2**), $SiMe_2Et$ (**3**), and $SiMe_2Ph$ (**4**).

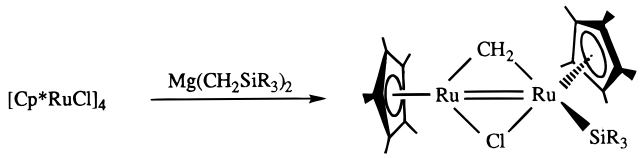

2, $SiR_3 = SiEt_3$
3, $SiR_3 = SiMe_2Et$
4, $SiR_3 = SiMe_2Ph$

The reactions must be performed at 0 °C because the products are thermally sensitive in solution. Dark red crystals of **2**−**4** are obtained in yields of 18−50%. The NMR data for **2**−**4** (Tables 1 and 2) correspond well with those reported for **1** and indicate that the structures of these new complexes are similar. In particular, the silyl group is terminal on one of the ruthenium atoms, so that the molecules possess no symmetry.

The ^{1}H NMR spectra of **2**−**4** at −90 °C show that the two protons of the bridging methylene group are diastereotopic: they appear at δ 10.27 and 10.78 for **2**, at δ 10.00 and 10.76 for **3**, and at δ 10.22 and 10.83 for **4**. The coupling between the two protons of the methylene ligand is too small to be observed. At this temperature, the two Cp* groups in each complex are inequivalent, as judged by the appearance of two singlets near δ 1.35 and 1.60. As we will show, these complexes engage in two dynamic processes: one that exchanges the inequivalent CH_2 protons of the bridging methylene group

(21) Other mechanisms include rotation of a terminal Ru−CH_2 group (see: Berry, D. H.; Bercaw, J. E. *Polyhedron* **1988**, *7*, 759−766), rotation around a Ru=Ru bond in an unbridged intermediate (see: Dyke, A. F.; Knox, S. A. R.; Mead, K. A.; Woodward, P. *J. Chem. Soc., Chem. Commun.* **1981**, 861−862), and a 180° twist of the tetrahedral metal center.

(22) Akita, M.; Hua, R.; Oku, T.; Tanaka, M.; Moro-oka, Y. *Organometallics* **1996**, *15*, 4162−4177.

(23) Osakada, K.; Koizumi, T.; Yamamoto, T. *Angew. Chem., Int. Ed. Engl.* **1998**, *37*, 349−351.

(24) Heine, A.; Stalke, D. *Angew. Chem., Int. Ed. Engl.* **1993**, *32*, 121−122.

(25) Hofmann, P.; Heiss, H.; Neiteler, P.; Müller, G.; Lachmann, J. *Angew. Chem., Int. Ed. Engl.* **1990**, *29*, 880−882.

Table 2. ^{13}C NMR Spectroscopic Data for 2−4[a]

assignment	2	3	4
$SiMe_2$		2.3 (q, $^1J_{CH}$ = 118)	0.4 (q, $^1J_{CH}$ = 118)
$SiMe_2$		3.4 (q, $^1J_{CH}$ = 118)	1.4 (q, $^1J_{CH}$ = 118)
$SiCH_2CH_3$	10.8 (t, $^1J_{CH}$ = 121)	14.6 (t, $^1J_{CH}$ = 118)	
$SiCH_2CH_3$	10.0 (q, $^1J_{CH}$ = 126)	9.2 (q, $^1J_{CH}$ = 124)	
C_5Me_5	9.1 (q, $^1J_{CH}$ = 128)	9.1 (q, $^1J_{CH}$ = 127)	8.7 (q, $^1J_{CH}$ = 128)
C_5Me_5	10.4 (q, $^1J_{CH}$ = 128)	10.5 (q, $^1J_{CH}$ = 127)	10.5 (q, $^1J_{CH}$ = 128)
C_5Me_5	80.3 (s)	80.4 (s)	80.7 (s)
C_5Me_5	93.1 (s)	93.3 (s)	93.2 (s)
p-CH			125.4 (d, $^1J_{CH}$ = 158)
m-CH			125.7 (d, $^1J_{CH}$ = 155)
o-CH			133.0 (d, $^1J_{CH}$ = 156)
i-C			149.5 (s)
CH_2	169.1 (t, $^1J_{CH}$ = 137)	169.9(t, $^1J_{CH}$ = 140)	170.6 (t, $^1J_{CH}$ = 141)

[a] All NMR spectra were taken at −93.5 °C in CD_2Cl_2. Chemical shifts are reported in ppm and coupling constants in Hz.

and another that exchanges the two inequivalent Cp* environments.

At low temperatures (−90 °C), the resonances for the silyl ligands in **2**−**4** confirm that no symmetry element passes through the Ru−Si bond. Thus, for the $SiEt_3$ complex **2**, the α-protons of the Si−Et groups are diastereotopic and give rise to two quartets at δ 0.94 and 1.01. For the $SiMe_2Et$ complex **3**, a similar situation pertains to the α protons of the Si−Et group except that the two α-H multiplets overlap to give a complex feature centered at δ 0.93. The two Si−Me groups should be diastereotopic also, but evidently the two resonances accidentally have the same chemical shift and give a singlet at δ 0.62. For the $SiMe_2Ph$ complex **4**, the two inequivalent Si−Me groups are distinguishable and resonate at δ 0.73 and 0.86.

In the low-temperature ^{13}C NMR spectra of compounds **2**, **3**, and **4**, the bridging methylene carbon appears as a triplet near δ 170 ($^1J_{CH}$ = 140 Hz). The inequivalence of the two Cp* groups is confirmed by the presence of two resonances for the quaternary carbons near δ 80 and 93 and two resonances for the methyl carbons at δ 9 and 10. The inequivalence of the Si−Me groups in the $SiMe_2Et$ and $SiMe_2Ph$ compounds **3** and **4** is confirmed by the appearance of two resonances for these groups in the ^{13}C NMR spectra.

Dynamic Behavior of 1−4 in Solution. The variable-temperature ^{1}H NMR spectra of **2**−**4** show that all of these complexes undergo two dynamic processes: a low-temperature process that exchanges the inequivalent Cp* groups and a high-temperature process that exchanges the diastereotopic protons of the bridging methylene ligand.

The two Cp* resonances seen in the ^{1}H NMR spectra at low temperature coalesce at approximately −60 °C for the $SiEt_3$ complex **2**, at about −75 °C for the $SiMe_2$-Et complex **3**, and at about −85 °C for the $SiMe_2Ph$ complex **4**. The two inequivalent CH_2 resonances seen for each compound at low temperature also coalesce, but do so at a higher temperature: 20 °C for **2**, 35 °C for **3**, and 50 °C for **4**. The experimental and computer-simulated spectra for the $SiEt_3$ complex **2** are compared in Figures 1 and 2 (see Supporting Information for analogous spectra of **3** and **4**).

For compounds **1**−**4**, Eyring plots of the Cp* exchange rate as a function of temperature are presented in Figure 3. Similar plots for the CH_2 exchange processes appear in Figure 4. The activation parameters for the dynamic processes in molecules **1**−**4** are collected in

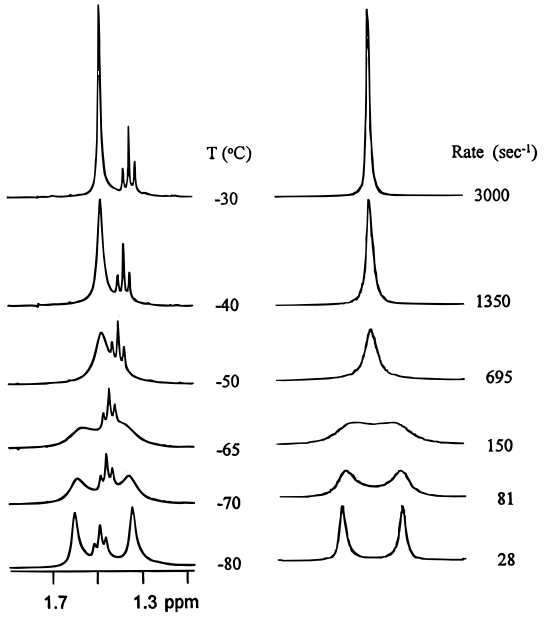

Figure 1. Variable-temperature 300 MHz ^{1}H NMR (left) and simulated (right) spectra of the Cp* protons in **2**. The triplet due to the $SiEt_3$ ligand has a temperature-dependent chemical shift.

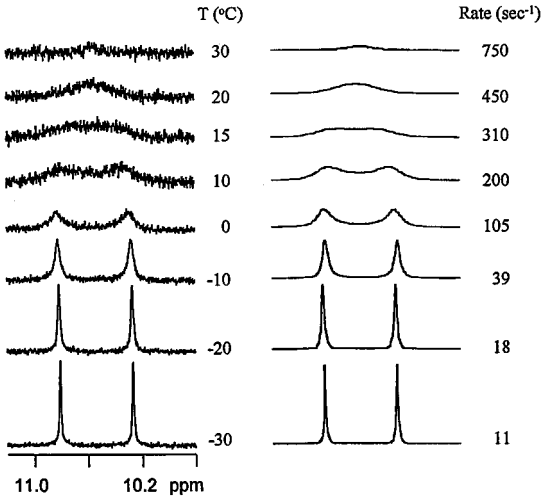

Figure 2. Variable-temperature 300 MHz ^{1}H NMR (left) and simulated (right) spectra of the bridging methylene protons in **2**.

Table 3 (Cp*) and Table 4 (CH_2). The activation parameters are clearly different for the two processes: $\Delta G^{\ddagger}$ at the coalescence temperature is approximately 9−10

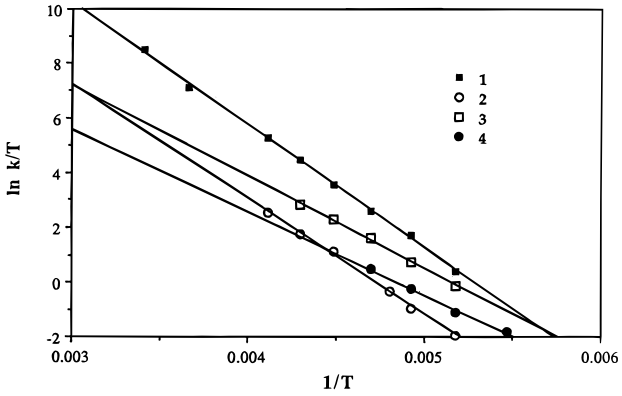

Figure 3. Eyring plots for the low-temperature Cp* exchange process in $Cp^*_2Ru_2(\mu\text{-}CH_2)(SiR_3)(\mu\text{-}Cl)$, where $SiR_3 = SiMe_3$ (**1**), $SiEt_3$ (**2**), $SiMe_2Et$ (**3**), and $SiMe_2Ph$ (**4**). Activation parameters are listed in Table 3.

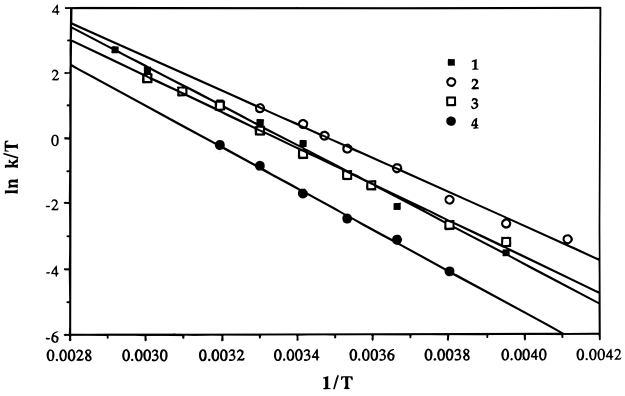

Figure 4. Eyring plots for the high-temperature μ-CH_2 exchange process in $Cp^*_2Ru_2(\mu\text{-}CH_2)(SiR_3)(\mu\text{-}Cl)$, where $SiR_3 = SiMe_3$ (**1**), $SiEt_3$ (**2**), $SiMe_2Et$ (**3**), and $SiMe_2Ph$ (**4**). Activation parameters are listed in Table 4.

Table 3. Activation Parameters for the Exchange of the Cp* Groups (via Metal-to-Metal Silyl Migration) in the $Cp^*_2Ru_2(\mu\text{-}CH_2)(SiR_3)(\mu\text{-}Cl)$ Complexes

cmpd	SiR_3	$\Delta H^{\ddagger}$ [a]	$\Delta S^{\ddagger}$ [b]	$\Delta G^{\ddagger}$ (200 K)[a]
1[c]	$SiMe_3$	9.0(2)	0.5(8)	8.9(1)
2	$SiEt_3$	8.3(3)	−7.8 (14)	9.9(1)
3	$SiMe_2Et$	6.6(4)	−13.0(17)	9.2(1)
4	$SiMe_2Ph$	6.0(4)	−18.0(21)	9.6(1)

[a] kcal mol^{-1}. [b] cal mol^{-1} K^{-1}. [c] Parameters from ref 20.

Table 4. Activation Parameters for the Exchange of the Methylene Protons (via Re-formation of the Silicon−Carbon Bond) in the $Cp^*_2Ru_2(\mu\text{-}CH_2)(SiR_3)(\mu\text{-}Cl)$ Complexes

cmpd	SiR_3	$\Delta H^{\ddagger}$ [a]	$\Delta S^{\ddagger}$ [b]	$\Delta G^{\ddagger}$ (300 K)[a]
1[c]	$SiMe_3$	12.0(3)	−7.0(10)	14.1(1)
2	$SiEt_3$	10.3(4)	−11.3(15)	13.7(1)
3	$SiMe_2Et$	11.0(3)	−10.4(12)	14.1(1)
4	$SiMe_2Ph$	12.5(6)	−7.7(20)	14.8(1)

[a] kcal mol^{-1}. [b] cal mol^{-1} K^{-1}. [c] Parameters from ref 20.

kcal/mol for the Cp* exchange process, but 14−15 kcal/mol for the CH_2 exchange process. More detailed comparisons of the activation parameters will be presented in the Discussion section (see below).

For the $SiMe_2Et$ and $SiMe_2Ph$ compounds **3** and **4**, the $SiMe_2$ groups are diastereotopic at low temperature, as are the α-protons of the Si−Et group in **3**. As the temperature is raised, these diastereotopic groups exchange also. The inequivalent SiEt α-protons in **3** appear as overlapping multiplets that coalesce to give a quartet at −70 °C. For **4**, the Si−Me groups also coalesce at −75 °C. The variable-temperature line shapes of the Si−Me resonances are compared to the computer-generated spectra in Figure 5. An Eyring plot (Figure 6) shows that the activation parameters for the Si−Me exchange process of $\Delta H^{\ddagger} = 5.8 \pm 0.3$ kcal mol^{-1} and $\Delta S^{\ddagger} = -19.2 \pm 1.6$ cal mol^{-1} K^{-1} are essentially identical to those for the Cp* exchange process (i.e., the low-temperature process) in **4**. Thus, we conclude that the same mechanism is responsible for both exchanges.

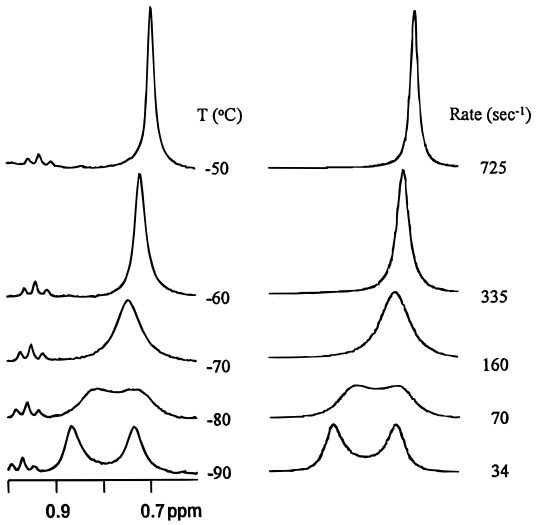

Figure 5. Variable-temperature 300 MHz ^{1}H NMR (left) and simulated (right) spectra of the $SiMe_2$ protons in **4**. The small triplet is due to an impurity. The downfield shifting of the $SiMe_2$ resonances at lower temperatures is probably the result of changes in the relative populations of $SiMe_2Ph$ rotamers.

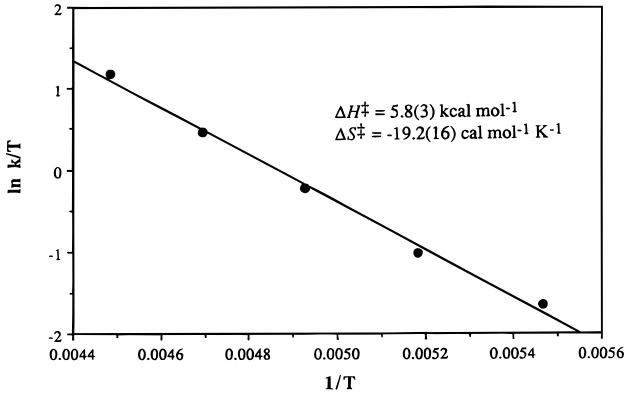

Figure 6. Eyring plot for the $SiMe_2$ exchange process in $Cp^*_2Ru_2(\mu\text{-}CH_2)(SiMe_2Ph)(\mu\text{-}Cl)$, **4**.

Discussion

Low-Temperature Dynamic Exchange Process. We have previously described the synthesis and characterization of the ruthenium methylene/silyl complex $Cp^*_2Ru_2(\mu\text{-}CH_2)(SiMe_3)(\mu\text{-}Cl)$, **1**.[20] In the present investigation, we have prepared analogues of **1** with different silyl groups; these include the $SiEt_3$, $SiMe_2Et$, and $SiMe_2Ph$ derivatives **2**−**4**. In all these complexes, the Cp* groups are inequivalent at low-temperature owing to the low molecular symmetry, but at temperatures

near −60 °C the ^{13}C NMR resonances for these groups coalesce owing to an exchange process. The low-temperature exchange process in **1**−**4** preserves the diastereotopic nature of the CH_2 protons, and from these results we conclude that an identical exchange mechanism (i.e., silyl hopping) operates in all four compounds. As proposed in our previous study, the only reasonable exchange mechanism is hopping of the SiR_3 group between ruthenium centers:

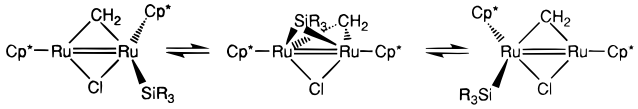

A comparison of the dynamic exchange rates in **1**−**4** provides an opportunity to determine how the silyl hopping process is affected by placing different substituents on the silicon atom. We find that the activation parameters for exchange of the Cp* environments in complexes **2**−**4** are generally similar to those measured previously for **1** (see Table 3). The activation parameters for **1**−**4** are not identical, however. At 200 K, the free energies of activation, $\Delta G^{\ddagger}$, increase in the order $SiMe_3$ (8.9 ± 0.05 kcal/mol) ≤ $SiMe_2Et$ (9.2 ± 0.05 kcal/mol) ≤ $SiMe_2Ph$ (9.6 ± 0.05 kcal/mol) < $SiEt_3$ (9.9 ± 0.05 kcal/mol).

The enthalpies and entropies of activation show an interesting dependence on the nature of the silyl substituents. The enthalpies of activation, $\Delta H^{\ddagger}$, decrease in the order $SiMe_3$ (9.0 ± 0.2 kcal/mol) ≥ $SiEt_3$ (8.3 ± 0.3 kcal/mol) > $SiMe_2Et$ (6.6 ± 0.4 kcal/mol) ≥ $SiMe_2Ph$ (6.0 ± 0.4 kcal/mol), whereas the entropies of activation, $\Delta S^{\ddagger}$, become more negative in the same order, $SiMe_3$ (0.5 ± 0.8 eu) > $SiEt_3$ (−7.8 ± 1.4 eu) > $SiMe_2Et$ (−13.0 ± 1.7 eu) > $SiMe_2Ph$ (−18.0 ± 2.1 eu). Neither of these series is correlated with the steric bulk of the silyl group;[26] instead, the enthalpies of activation are the smallest and the entropies of activation are the most negative for the complexes (**3** and **4**) that bear the nonsymmetrically substituted silyl ligands $SiMe_2Et$ and $SiMe_2Ph$. Evidently, for complexes **3** and **4**, there is an especially large increase in order upon proceeding from the ground state to the transition state.

Similar but less dramatic variations in activation parameters have been seen in some other reactions of nonsymmetrically substituted silane species. For example, an investigation of the kinetics of oxidative addition of tertiary silanes to the $CpMn(CO)_2$ fragment showed that the activation parameters for the symmetrically substituted silanes $HSiEt_3$, $HSi(n\text{-}Pr)_3$, $HSi(i\text{-}Pr)_3$, and $HSiPh_3$ were nearly identical, but that $\Delta H^{\ddagger}$ was 1 kcal mol^{-1} smaller and $\Delta S^{\ddagger}$ was 2 cal mol^{-1} K^{-1} more negative for the nonsymmetrically substituted silane, $HSiMe_2Et$.[27]

In the $SiMe_2Et$ and $SiMe_2Ph$ derivatives **3** and **4**, the two Si−Me groups are inequivalent at low temperatures, and one interesting question is whether silyl hopping is accompanied by exchange of the Si−Me groups. We find that the two Si−Me resonances seen for **4** at low temperatures coalesce as the sample is warmed. The activation parameters for this process are essentially identical to those measured for exchange of the Cp* environments, and we conclude that the low-temperature exchange process also permutes the Si−Me groups. This finding is consistent with the silyl hopping mechanism: the two Si−Me groups must be permuted as long as the silyl group remains on the same side of the $Ru_2(\mu\text{-}CH_2)(\mu\text{-}Cl)$ unit and the stereochemistry at silicon[17] is not inverted during the hopping process. The exchange of the methyl groups is depicted in the drawing below: methyl group A is initially in the site closer to the chloride ligand but ends up in the site closer to the methylene ligand after migration (and vice versa for methyl group B):

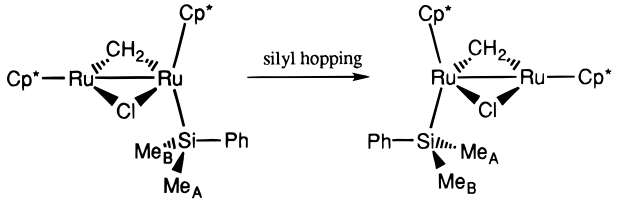

Although the above drawing depicts rotamers in which the phenyl substituent is anti to the Ru−Ru bond, silyl hopping effects exchange of Me_A and Me_B irrespective of the actual rotameric conformations adopted.

We now ask, why are the activation entropies more negative for the $SiMe_2Et$ and $SiMe_2Ph$ complexes **3** and **4**? If the silyl groups bear identical substituents (as in **1** and **3**), there will be three degenerate pathways for silyl hopping, each pathway corresponding to a different rotameric permutation of the three identical substituents. For compounds **3** and **4**, which possess nonsymmetrically substituted silyl groups, it is likely, either for steric reasons or to satisfy the principle of microscopic reversibility, that the pathway corresponding to the lowest energy transition state for silyl hopping involves only one of the three possible rotamers. As a result, the transition state for silyl hopping of the nonsymmetrically substituted silyl groups would be more ordered, and the activation entropy will be more negative by the statistical factor $-R \ln 3 = -2.2$ eu. This statistical factor, however, is insufficient to account for the 6−10 eu more negative activation entropies seen for **3** and **4**.

Another possible explanation of the trend in activation entropies is that the transition states are relatively crowded and that several internal conformational degrees of freedom are lost. The presence of three bridging groups in the transition state would certainly increase the degree of steric crowding relative to that present in the doubly bridged ground-state structure. Also possible is that solvent reorganization effects contribute to the activation entropies, and the nonsymmetrically substituted silyl groups are likely to cause a greater increase in solvent reorganization than the symmetrically substituted groups. The $SiMe_2Ph$ derivative **4** shows the most negative $\Delta S^{\ddagger}$, a fact that suggests the presence of especially strong solvent interactions in this case, possibly involving arene−arene stacking interactions between the Si−Ph group and the toluene-d_8 molecules of the solvent.

High-Temperature Exchange Process. Our previous studies of the ruthenium methylene/silyl complex $Cp^*_2Ru_2(\mu\text{-}CH_2)(SiMe_3)(\mu\text{-}Cl)$, **1**, showed that the CH_2

(26) Tolman, C. A. *Chem. Rev.* **1977**, *77*, 313−348. The cone angles of the silyl groups were assumed to be similar to those of similarly substituted phosphine ligands.

(27) Hill, R. H.; Wrighton, M. S. *Organometallics* **1987**, *6*, 632−638.

protons of the bridging methylene group are inequivalent at low temperature, but at 45 °C these two resonances coalesce owing to a second fluxional process.[20] Of several possible mechanisms that could account for this exchange process, in our previous study we ruled out all but one: reversible re-formation of the C−Si bond between the methylene and silyl groups.

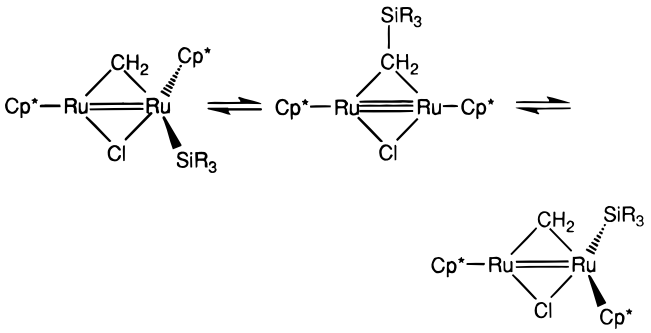

The activation parameters for this high-temperature process are nearly identical for compounds **1**−**4** (Table 4). This finding suggests that the transition state for migration of the silyl ligand to the methylene group is not highly crowded and that the solvent reorganization term is relatively insensitive to the nature of the substituents on silicon.

Conclusions. Analogues of $Cp^*_2Ru_2(\mu\text{-}CH_2)(SiMe_3)(\mu\text{-}Cl)$ have been synthesized in which the silicon atom bears different substituents. ^1H NMR studies reveal that these new complexes all undergo two different exchange processes. The activation parameters for the low-temperature process, migration of the silyl group from one metal to the other, are sensitive to the nature of the substituents on silicon: $\Delta H^‡$ becomes smaller and $\Delta S^‡$ becomes more negative if the substituents are nonidentical or are larger. Solvent reorganization effects may contribute to the observed variations in the $\Delta S^‡$ values. The activation parameters for the high-temperature process, reversible Si−C bond formation, are largely independent of the nature of the silyl substituents, at least for the substituents we studied (Me, Et, and Ph).

Experimental Section

All operations were performed under vacuum or under argon by using Schlenk and cannula methods. Solvents were distilled from sodium benzophenone (pentane, diethyl ether, tetrahydrofuran) immediately before use. The tetramer $[Cp^*RuCl]_4$[28] and the dialkylmagnesium reagents[29,30] $Mg(CH_2SiEt_3)_2$, $Mg(CH_2SiMe_2Et)_2$, and $Mg(CH_2SiMe_2Ph)_2$ were prepared according to literature methods. Dichloromethane-d_2 (Cambridge Isotope Laboratories) and toluene-d_8 (Cambridge Isotope Laboratories) were used as received. IR spectra were recorded on a Nicolet Impact 410 Fourier transform infrared spectrometer as Nujol mulls between KBr salt plates. The ^1H NMR spectra were recorded at 300 MHz on a General Electric QE-300 spectrometer. The ^{13}C NMR spectra were recorded at 125 MHz on a Varian UI500WB spectrometer. Chemical shifts are reported in δ units (positive shifts to high frequency) relative to TMS. Low-resolution field desorption (FD) mass spectra were obtained on a Finnigan-MAT 731 mass spectrometer, and low-resolution fast atom bombardment (FAB) mass spectra were obtained on a VG ZAB-SE mass spectrometer. Microanalyses were performed by the University of Illinois School of Chemical Sciences Microanalytical Laboratory.

Simulations of the dynamic NMR spectra were carried out using the program DNMR, which is available from the Quantum Chemistry Program Exchange. Line widths at half-intensity were determined from the NMR spectra and were used to measure the transverse relaxation times (T_2). The rates of exchange as a function of temperature were determined from visual comparisons of experimental spectra with computed trial line shapes. The errors in the rate constants of ca. 10% were estimated on the basis of subjective judgments of the sensitivities of the fits to changes in the rate constants. The temperature of the NMR probe was calibrated using methanol (for low temperatures) and ethylene glycol (for high temperatures),[31,32] and the estimated relative error in the temperature measurements was 0.3 K. The activation parameters were calculated from the Eyring equation by using a linear least-squares procedure contained in the program Passage, which is available from Passage Software, Inc. The errors in $\Delta H^‡$ and $\Delta S^‡$ were computed from error propagation formulas which we have described elsewhere;[33] the errors in $\Delta G^‡$ were computed from the propagation formula:

$$(\sigma\Delta G^‡)^2 = R^2T^2\left[\left(\frac{\sigma T}{T}\right)^2\left(1 + \ln\frac{k_BT}{kh}\right)^2 + \left(\frac{\sigma k}{k}\right)^2\right]$$

Bis(pentamethylcyclopentadienyl)(μ-chloro)(μ-methylene)(triethylsilyl)diruthenium(III), $Cp^*_2Ru_2(\mu\text{-}CH_2)(SiEt_3)(\mu\text{-}Cl)$ (2). An orange slurry of $[Cp^*RuCl]_4$ (0.25 g, 0.23 mmol) in diethyl ether (35 mL) at 0 °C was treated with $Mg(CH_2SiEt_3)_2$ (2.9 mL of a 0.10 M solution in diethyl ether, 0.29 mmol). The solution color turned dark red immediately. The solution was stirred at 0 °C for 1 h, the solvent was removed under vacuum, and the residue was extracted with cold pentane (3 × 20 mL) at 0 °C. The combined extracts were filtered, concentrated to 25 mL, and cooled to −20 °C to afford dark red crystals of **2**. Yield: 0.1214 g (41%). Mp: 145 °C. Anal. Calcd for $C_{27}H_{47}ClRu_2Si$: C, 50.9; H, 7.43; Cl, 5.56; Ru, 31.7. Found: C, 50.8; H, 7.59; Cl, 5.76; Ru, 30.2. MS: *m/e* 638 (M^+). IR (cm^{-1}): 1236 (vw), 1221 (w), 1072 (vw), 1024 (m), 1004 (w), 828 (m), 701 (w), 669 (w), 659 (w), 614 (vw), 460 (vw).

Bis(pentamethylcyclopentadienyl)(μ-chloro)(μ-methylene)(ethyldimethylsilyl)diruthenium(III), $Cp^*_2Ru_2(\mu\text{-}CH_2)(SiMe_2Et)(\mu\text{-}Cl)$ (3). An orange slurry of $[Cp^*RuCl]_4$ (0.25 g, 0.23 mmol) in diethyl ether (25 mL) at 0 °C was treated with $Mg(CH_2SiMe_2Et)_2$ (3.8 mL of a 0.075 M solution in diethyl ether, 0.29 mmol). The solution color turned dark red after ∼30 s. The solution was stirred at 0 °C for 4.5 h, the solvent was removed under vacuum, and the residue was extracted with cold pentane (2 × 50 mL) at 0 °C. The combined extracts were concentrated to 40 mL, filtered, concentrated further to 15 mL, and cooled to −20 °C to afford dark red crystals of **3**. Yield: 0.1400 g (50%). Mp: 164 °C. Anal. Calcd for $C_{25}H_{43}ClRu_2Si$: C, 49.3; H, 7.11; Cl, 5.82; Ru, 33.2. Found: C, 49.3; H, 7.21; Cl, 5.65; Ru, 35.9. MS: *m/e* 609 (M^+). IR (cm^{-1}): 1229 (w), 1220 (m), 1071 (vw), 1023 (m), 1011 (w), 961 (vw), 943 (w), 821 (m), 804 (m), 792 (m), 744 (vw), 734 (vw), 668 (w), 659 (w), 633 (vw), 595 (m), 462 (w), 451 (vw).

Bis(pentamethylcyclopentadienyl)(μ-chloro)(μ-methylene)(phenyldimethylsilyl)diruthenium(III), $Cp^*_2Ru_2(\mu\text{-}CH_2)(SiMe_2Ph)(\mu\text{-}Cl)$ (4). A mixture of $[Cp^*RuCl]_4$ (0.25 g, 0.23 mmol) and $Mg(CH_2SiMe_2Ph)_2$ (0.11 g, 0.35 mmol) was

(28) (a) Fagan, P. J.; Mahoney, W. S.; Calabrese, J. C.; Williams, I. D. *Organometallics* **1990**, *9*, 1843−1852. (b) Fagan, P. J.; Ward, M. D.; Calabrese, J. C. *J. Am. Chem. Soc.* **1989**, *111*, 1698−1719.

(29) Andersen, R. A.; Wilkinson, G. *Inorg. Synth.* **1979**, *19*, 262−265.

(30) Decker, Q. W.; Post, H. W. *J. Org. Chem.* **1960**, *25*, 249−252.

(31) Friebolin, H.; Schilling, G.; Pohl, L. *Org. Magn. Reson.* **1979**, *12*, 569−573.

(32) Van Geet, A. L. *Anal. Chem.* **1970**, *42*, 679−680.

(33) Morse, P. M.; Spencer, M. D.; Wilson, S. R.; Girolami, G. S. *Organometallics* **1994**, *13*, 1646−1655.

dissolved in tetrahydrofuran (18 mL) at 0 °C to give a dark red solution. After the solution had been stirred at 0 °C for 1.5 h, a solution of $Mg(CH_2SiMe_2Ph)_2$ (0.11 g, 0.35 mmol) in tetrahydrofuran (5 mL) was added. The resulting mixture was stirred for 1.5 h at 0 °C. The solvent was removed under vacuum, the residue was dissolved in cold diethyl ether (20 mL) at 0 °C, and then the diethyl ether was removed under vacuum. The residue was extracted with cold pentane (4 × 30 mL) at 0 °C. The combined extracts were filtered, concentrated to 10 mL, and cooled to −20 °C to afford dark red gummy microcrystals. The crude product was recrystallized from pentane (10 mL) at −20 °C. Yield: 0.0535 g (18%). Mp: 113 °C. Anal. Calcd for $C_{29}H_{43}ClRu_2Si$: C, 53.0; H, 6.59; Cl, 5.39; Ru, 30.7. Found: C, 52.4; H, 6.38; Cl, 4.99; Ru, 28.0. MS: *m*/*e* 657 (M^+). IR (cm^{-1}): 1482 (w), 1425 (m), 1249 (vw), 1234 (w), 1222 (w), 1116 (vw), 1097 (m), 1070 (w), 1024 (m), 826 (m), 804 (m), 795 (m), 789 (m), 731 (m), 703 (w), 641 (vw), 475 (vw).

NMR Tube Experiments. A typical NMR sample was prepared in the following way. A 0.02 g sample of **2** was dissolved in toluene-d_8 (1 mL) at 0 °C. This solution was transferred to an argon-flushed 5 mm NMR tube at 0 °C. The cold NMR sample was placed into a precooled (−90 °C) NMR probe. Spectra were recorded after the sample had been kept at the desired temperature for 15 min.

Acknowledgment. We thank the Department of Energy under Grant DEFG02-96ER45439 for support of this work. NMR spectra were obtained at the Varian Oxford Instrument Center for Excellence in NMR Laboratory. Funding for this instrumentation was provided in part from the W. M. Keck Foundation, the National Institutes of Health (PHS 1 S10 RR10444-01), and the National Science Foundation (NSF CHE 96-10502).

Supporting Information Available: Figures of the experimental and computer-simulated line shapes for the variable-temperature NMR spectra of **3** and **4** in the Cp* and bridging CH_2 regions. This material is available free of charge via the Internet at http://pubs.acs.org.

OM990156B